Biomolecular activity switch : an application of metallic nanoparticle plasmon resonance

J. Alper[*], A. Wijaya[**], M. Crespo[***], L. DeFlores[****],
A. Tokmakoff[****] and K. Hamad-Schifferli[*,***]

[*]Massachusetts Institute of Technology, Department of Mechanical Engineering,
77 Massachusetts Ave. Building 56-367, Cambridge, MA 02139, USA, jalper@mit.edu
[**]Massachusetts Institute of Technology, Department of Chemical Engineering, Cambridge, MA, USA
[***]Massachusetts Institute of Technology, Department of Biological Engineering, Cambridge, MA, USA
[****]Massachusetts Institute of Technology, Department of Chemistry, Cambridge, MA, USA

ABSTRACT

For devices both technological and biomedical, scientists and engineers are interested in designing molecular machines for a variety of tasks. Most promising are modified natural systems or artificial systems comprised of natural proteins. To harness the potential of these nanoscale machines it is necessary to exert specific, external control. In this paper, we propose a simple control method, a biomolecular activity switch, which takes advantage of the optical properties of gold nanoparticles and the structure-function relationship of proteins. We demonstrate the viability of using ultrafast-pulsed laser irradiation on gold nanorods as a biomolecular switch. We show how the unique properties of these nanoparticles enable this method. This has implications on not only biomolecular control, but also delivery applications.

Keywords: gold nanorod, ultrafast laser, biomolecular control, controlled release, conjugation

1 INTRODUCTION

We examine the possibility of using ultrafast laser pulses and gold nanorods (AuNRs) to control the activity of biomolecules. We demonstrate that possibility using octadecyl rhodamine B chloride (R_{18}) as a model for a biomolecule, with its intrinsic fluorescence as a model for activity.

In recent years, scientists and engineers have been interested in designing molecular machines for a variety of tasks. Most promising are systems that exploit nature's building blocks, either modified natural systems or artificial systems comprised of natural proteins [1]. Nature controls these biomolecular systems by chemical, mechanical, thermodynamic or even electrical means. However, for scientists to harness the full potential of these nanoscale machines it is necessary to control them externally.

Many studies address controlling molecular machinery at the macromolecular scale. The techniques they employ generally imitate nature, and include chemical [2], direct electrical [3, 4], laser induced thermal [5-7], direct thermal [8, 9] and photoactivated [10] control techniques. Though most try for the relatively simple "on/off" control mechanism, none of these systems is ideal.

There are three hallmarks of an ideal on/off biomolecular control mechanism: specific, local, and external. Specificity allows targeting a particular molecule within a system. Locality ensures that only the intended target is affected. Externality allows integration of the control mechanism into a larger system of control.

To meet these hallmarks, we need to affect the targeted biomolecule specifically. Gold nanoparticles (AuNPs) are a promising material to interface between the macro and nano size scales due to their nanometer size, ability to preserve biological activity and unique optical properties. Gold particles are successfully used in a number of biomolecular applications, including DNA delivery [11], DNA antisense amplification [12], sensing amplification [13, 14] and imaging [15]. AuNPs' chemical nature enables site-specific conjugation to proteins, which is key to maintaining the structure and function of conjugated proteins [16]. AuNPs are also used in other biomolecular control techniques including dehybridizing DNA with radio frequency magnetic fields [17], permanently denaturing proteins [18] and gene regulation [11].

We propose a simple control technique that addresses all the hallmarks of an ideal biomolecular control system. We propose a biomolecular activity switch that takes advantage of the optical properties of gold nanoparticles, the structure-function relationship of proteins and some of nature's control systems. The technique consists of a biomolecule conjugated to a nanoparticle. The conjugate is exposed to an electromagnetic wave. The nanoparticle focuses and converts the wave's energy into heat that is then conducted into the attached biomolecule. This causes a change in the biomolecule that reverses the activity of a critical component of a biomolecular system. Thus, the biological system's activity is actuated by this change.

We propose three models for control, but in this paper we discuss and demonstrate a proof of concept for just one, the protein release model for biomolecular control. In the

protein release model, the target protein is loosely bound to the particle that suppresses its activity. When the system is exposed to an electromagnetic field, the protein is released, and its activity is restored. This flips the activity of larger molecular system for which it is a part. In lieu of an actual protein in a complex biomolecular system, we have conjugated a fluorophore, rhodamine red, to a gold nanorod. When conjugated, the activity of the fluorophore, its ability to fluoresce, is suppressed because the gold nanorod acts as a strong quencher [19].

Gold nanorods have recently drawn the interest of a number of scientific communities. Generally, AuNRs are interesting because of their unique optical properties. It is widely known that gold nanoparticles have an optical absorption peak due to a surface plasmon resonance near 520 nm. The surface plasmon resonance is a result of the coherence of all the free electrons in the nanoparticle's conduction band that leads to an in phase oscillation of the electron cloud. For gold nanoparticles larger than 10 nm, this corresponds to a large optical absorption at the oscillation frequency [20]. As the shape changes from a spherical nanoparticles to rod-like nanoparticles, the absorption peak due to the surface plasmon resonance splits in two. One peak, due to the transverse surface plasmon resonance, remains near 520 nm. The other, due to the longitudinal plasmon, red shifts as the AuNR's aspect ratio (length/diameter) increases [20].

Gustav Mie was the first to explain the absorbing properties of small gold nanoparticles by solving Maxwell's equations [21]. His theory relates the extinction cross section of a particle to the dielectric functions of the particle and its immediate surroundings, the volume of the particle and the frequency of the incident light under the dipole approximation. The theory was extended to account for particles elongated along an axis by Richard Gans a few years later [22]. Gans' result shows that the AuNR's aspect ratio controls the wavelength of the absorption peak.

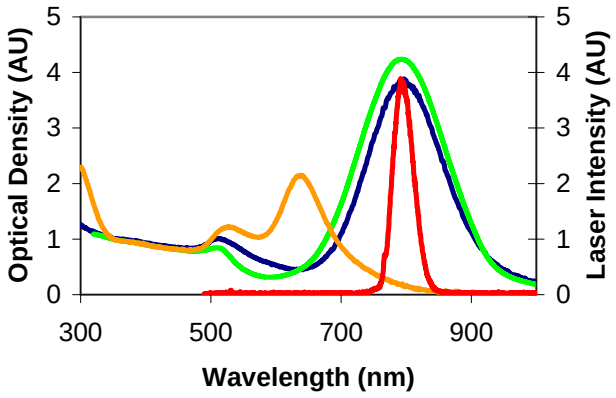

Figure 1: Optical absorption of AuNRs. Blue line – large aspect ratio AuNRs. Orange line – small aspect ratio AuNRs. Green line – Mie-Gans theory based on size analysis of large aspect ratio AuNRs (figure 3). Red line – Spectral output of laser

To heat these AuNRs, we excite the longitudinal plasmon resonance using a home-built Ti:sapphire laser pumping an optical parametric amplifier. Each emitted pulse has maximum of 650 μJ of energy, a duration of 40 fs, and repeat at a frequency of 1 kHz. The laser's spectral output peak at 800 nm coincides with the longitudinal plasmon absorption peak of large aspect ratio AuNRs, but it has little overlap with the absorption peak of the small aspect ratio AuNRs (figure 1). We chose to use 800 nm light because it is within the "tissue window" where most biological materials and water do not have high absorbance. This allows us to heat the AuNRs but not other components including the R_{18}. At 790 nm, the R_{18}'s extinction coefficient of is 7 orders of magnitude lower than AuNR's. An ultrafast laser is necessary to achieve high thermal confinement [23]. The temperature rise of the targeted protein is significant, while just a few nanometers away it is negligible (figure 2, inset).

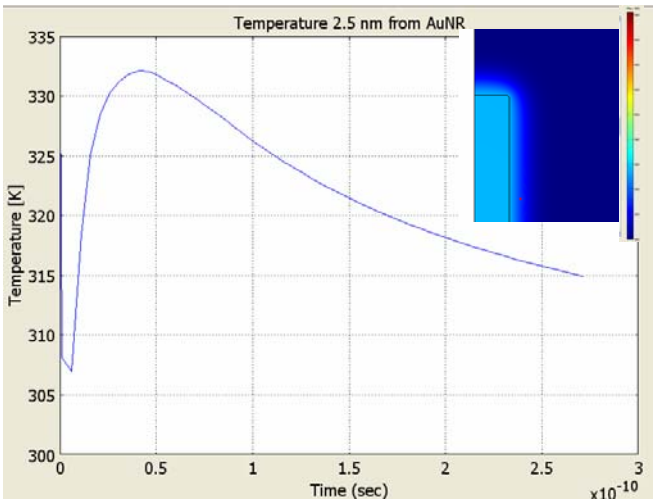

Figure 2: Model of AuNR heating due to ultrafast laser pulse. The temperature just outside the AuNR (d=2.5 nm) is a strong function of time, and the temperature rise is significant. The inset shows the spatial distribution of heat 40 fs after the laser pulse near an AuNR.

We modeled the induction of heat in the AuNR and the transfer of that heat to conjugated proteins using Mie-Gans theory, a two-temperature model of AuNR thermalization and continuum heat transfer through the solvent (figure 2). Based on these models, we performed a series of experiments as a proof of concept for the biomolecular activity switch detailed in the following sections.

2 MATERIALS AND METHODS

We synthesized AuNRs by a modified non-seeding method [24] with final chemical concentrations noted in table 1. Hexadecyltrimethylammonium bromide (CTAB) 99% pure is dissolved into a saline solution. To this, gold(III) chloride trihydrate ($HAuCl_4$ $3H_2O$) and silver

nitrate ($AgNO_3$) are added and the yellow-brown solution is agitated lightly. L-ascorbic acid (AA) is added and the solution turns clear upon inversion agitation. Sodium borohydride ($NaBH_4$) is added and the solution is again agitated by inversion. The solution is incubated at room temperature for 3 hours. During this time, the solution changes to a deep purple/brown. At this point, the AuNR solution is washed by centrifugation to remove excess CTAB and other non-reacted reagents. It is concentrated to a final concentration of 100 nM AuNRs and 1 mM CTAB for storage.

	CTAB (mM)	NaCl (mM)	$HAuCl_4$ (mM)	$AgNO_3$ (μM)	AA (mM)	$NaBH_4$ (μM)
1	150	2.25	0.9	135	1.8	1
2	100	7.5	2.25	400	5	2

Table 1: Concentrations of reagents for AuNR synthesis. Sample 1 yields large aspect ratio AuNRs. Sample 2 yields small aspect ratio AuNRs.

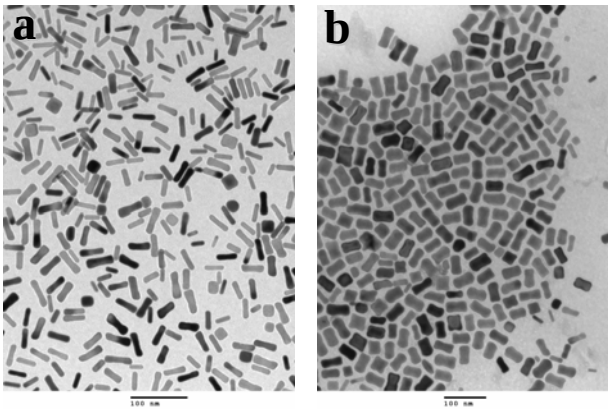

Figure 3: a) TEM of large aspect ratio AuNRs. Length = 34.9 ± 7.4 nm. Diameter = 10.3 ± 2.6 nm. Aspect ratio = 3.5 ± 0.7. b) Small aspect ratio AuNRs. Length = 48.0 ± 7.7 nm. Diameter = 21.5 ± 3.9 nm. Aspect ratio = 2.3 ± 0.4. Scale bar on both images is 100 nm

We conjugated octadecyl rhodamine B chloride to AuNRs using the hydrophobic interaction between the octadecylane tail and the CTAB bilayer on the AuNRs. The R_{18} is dissolved in DMSO and added to a solution of 10 nM AuNRs and 1 mM CTAB in a molar ratio of 500:1 R_{18} to AuNR. The samples are incubated at room temperature overnight. Finally, the AuNR-R_{18} conjugates are washed and concentrated to a final concentration of 100 μM CTAB and 10 nM AuNR-R_{18}. Leaving the CTAB concentration at 100 μM eliminates CTAB micelles. The critical micelle concentration of CTAB is approximately 0.5 to 1.1 mM [25, 26]. This minimizes the R_{18} free in solution because CTAB micelles make soluble the otherwise insoluble R_{18}.

We characterized the control technique with R_{18} release experiments. AuNR-R_{18} conjugates are diluted to 1 nM in ddH_2O. The concentration of CTAB is raised to 10 mM. Then the sample is split in two. The first half of the sample, is set aside at room temperature. The second half is either bulk heated in a water bath, or irradiated with laser pulses. Next, AuNRs in both halves of the sample are separated from the supernatant by centrifugation. The fluorescence of the supernatant is measured and the amount of R_{18} present in each half of the sample is compared. Differences in the fluorescence are directly related to differences in the rate of R_{18} release from the AuNR into the CTAB micelles between the halves of the sample.

To control for the locality of the laser effects, we measured the bulk temperature rise of the samples during laser irradiation. AuNR-R_{18} conjugates are prepared just as in R_{18} release experiments. The sample's temperature is recorded as a function of time and compared to an equal volume sample without AuNRs. The bulk temperature rise of the sample is quantified for various AuNR-R_{18} concentrations.

3 RESULTS AND DISCUSSION

Laser Exposure Time (min)	I_{Rel}/I_{Bl} at 440 μJ/cm^2	I_{Rel}/I_{Bl} at 330 μJ/cm^2	I_{Rel}/I_{Bl} at 220 μJ/cm^2
1	-0.16	0.11	-0.11
5	-0.32	0.17	0.04
20	-0.44	0.29	-0.18

Table 2: Results of R_{18} laser release experiment with large aspect ratio AuNRs. I_{Rel}/I_{Bl} is the difference in fluorescence intensity (559 nm excitation, 583 nm emission) between the supernatant of laser irradiated sample and the half that was not irradiated (I_{Rel}) normalized by the fluorescence intensity of the supernatant of the half that was not irradiated (I_{Bl}). Experiments were done at 220, 330 and 440 μJ/cm^2 laser fluence per pulse.

The primary result (table 2) of this study is that at low laser fluence, 220 μJ/cm^2, there is no significant change in the release rate of R_{18} from the AuNRs as compared to the sample not exposed to the laser. At medium power, 330 μJ/cm^2, there is an increasing amount of R_{18} released. At the highest laser power, 440 μJ/cm^2, the fluorescence intensity of the supernatant is significantly lower than it was for samples not exposed to the laser. A fluence of 440 μJ/cm^2 per pulse is high enough to melt the AuNRs. A temperature high enough to melt AuNRs is likely to be high enough to damage the R_{18} irrecoverably.

To ensure the release effect is due to AuNRs' light absorbing properties, we repeated the R_{18} release experiment with small aspect ratio nanorods. These AuNRs do not have an absorption peak at 790. The smaller aspect ratio (figure 3) causes a blue shift of the longitudinal plasmon resonance to 634 nm (figure 1). From figure 1 we see the absorption cross section at 790 nm for small aspect ratio AuNRs is about 5% of that for high aspect ratio

AuNRs. We see in table 2 that the effect of the laser on small aspect ratio AuNR-R_{18} conjugates is dramatically different from those with large aspect ratios. Here there is no difference between the release rate of R_{18} in samples irradiated by the laser (table 3) and the release rate of R_{18} in samples not irradiated.

Laser Exposure Time (min)	I_{Rel}/I_{Bl} at 440 $\mu J/cm^2$	I_{Rel}/I_{Bl} at 330 $\mu J/cm^2$	I_{Rel}/I_{Bl} at 220 $\mu J/cm^2$
1	0.10	-0.09	-0.21
5	-0.06	-0.13	0.04
20	-0.08	0.03	0.02

Table 3: Results of R_{18} laser release experiment with small aspect ratio AuNRs. Both the type of data in this table, and the experimental conditions under which they were collected match the data in Table 2.

To ensure the results of the R_{18} release experiments are not due to bulk heating of the solution we measured the temperature of the sample while we exposed it to the laser. The temperature of the sample rises 0.5 C above room temperature. When we increased the concentration of AuNRs, the temperature rise increased (data not shown). Then we repeated the R_{18} release experiment using a 30 C water bath to bulk heat the sample in stead of the laser. There was no perceptible acceleration of release due to elevating temperature about 7 C. This result indicated that the effects we report above are not due to a global heating effect of the laser, rather due to a local heating effect.

4 CONCLUSIONS

The results from this study demonstrate the viability of an ultrafast laser-AuNR system to control the activity of a biomolecule and the potential to actuate the activity of biomolecular machine. These results also highlight some of the physical and practical limits of this control mechanism. There is a limit on the aspect ratio of the AuNRs to maintain sensitivity to the laser. Based on Mie-Gans theory and our experiments, the aspect ratio must be within about 0.5 of the target to maintain an optical absorption peak that significantly overlaps the laser. There is a limit on the concentration of AuNRs before bulk heating becomes an issue. Any more than 1-2 nM AuNRs will cause bulk heating that can disrupt the biomolecular system. There is a limit on the fluence to cause release. Too little and there will be no release and too much and the AuNR-biomolecule conjugate may become hot enough to destroy either component.

The principles demonstrated here can be applied to a number of biomolecular control mechanism along with possible drug deliver applications.

5 ACKNOWLEDGEMENTS

We would like to thank the CMSE Electron Microscopy Lab at MIT for use of the TEM and the Krystyn van Vliet Lab for the use of their UV-Vis spectrophotometer.

REFERENCES

1. Kay, E.R., D.A. Leigh, and F. Zerbetto, Angewandte Chemie - International Edition, 2007. **46**(1-2): p. 72.
2. Liu, H., et al., Nat Mater, 2002. **1**(3): p. 173.
3. Mihajlovic, G., et al., Applied Physics Letters, 2004. **85**(6): p. 1060.
4. Wong, I.Y., M.J. Footer, and N.A. Melosh,. Soft Matter, 2007. **3**(3): p. 267.
5. Kato, H., et al., Proceedings of the National Academy of Sciences, 1999. **96**(17): p. 9602.
6. Kawaguchi, K. and S.i. Ishiwata, Cell Motility and the Cytoskeleton, 2001. **49**(1): p. 41.
7. Reinhardt, H., et al., Lab on a Chip, 2007. **7**(11): p. 1509.
8. Peng, T., C. Dohno, and K. Nakatani, ChemBioChem, 2007. **8**(5): p. 483.
9. Pennadam, S.S., et al., J. Am. Chem. Soc., 2004. **126**(41): p. 13208.
10. Mayer, G. and A. Heckel, Angewandte Chemie International Edition, 2006. **45**(30): p. 4900.
11. Chen, C.C., et al., J. Am. Chem. Soc., 2006. **128**(11): p. 3709.
12. Rosi, N.L., et al., Science, 2006. **312**(5776): p. 1027.
13. Taton, T.A., C.A. Mirkin, and R.L. Letsinger, Science, 2000. **289**(5485): p. 1757.
14. Katz, E. and I. Willner, Angewandte Chemie International Edition, 2004. **43**(45): p. 6042.
15. Sokolov, K., et al., Cancer Res, 2003. **63**(9): p. 1999.
16. Aubin-Tam, M.-E. and K. Hamad-Schifferli, Langmuir, 2005. **21**(26): p. 12080.
17. Hamad-Schifferli, K., et al., Nature, 2002. **415**(6868): p. 152.
18. Huettmann, G., et al. 2003. Munich, Germany: The International Society for Optical Engineering.
19. Dulkeith, E., et al., Physical Review Letters, 2002. **89**(20): p. 203002.
20. Link, S. and M.A. El-Sayed, International Reviews in Physical Chemistry, 2000. **19**(3): p. 409.
21. Mie, G., Annalen der Physik, 1908. **330**(3): p. 377-445.
22. Gans, R., Ann Phy, 1912. **342**(5): p. 881-900.
23. Huettmann, G. and R. Birngruber, IEEE J of Selected Topics in Quantum Electronics, 1999. **5**(4): p. 954.
24. Jana, N.R.,. Small, 2005. **1**(8-9): p. 875-882.
25. Bahri, M.A., et al., Colloids and Surfaces A: Physicochemical and Engineering Aspects, 2006. **290**(1-3): p. 206.
26. Tedeschi, A.M., et al., Physical Chemistry Chemical Physics, 2003. **5**(19): p. 4204.
27. Aubin, M.-E., D.G. Morales, and K. Hamad-Schifferli, Nano Letters, 2005. **5**(3): p. 519.